Available online at www.sciencedirect.com
ScienceDirect
Journal of the European Ceramic Society 28 (2008) 1–13
www.elsevier.com/locate/jeurceramsoc

An estimation of ceramic fracture at singularities by a statistical approach

J. Laurencin [a,*], G. Delette [a], M. Dupeux [b]

[a] CEA/LITEN/DTH/LEV, 17 avenue des martyrs, 38054 Grenoble, France
[b] SIMAP (INP Grenoble/CNRS/UJF), BP 75 38402 Saint Martin d'Hères, France

Received 22 March 2007; received in revised form 23 May 2007; accepted 2 June 2007
Available online 6 August 2007

Abstract

A statistical analysis based on weakest link theory is employed to describe the brittle fracture induced at singularities in ceramic materials. Relationships are stated between the Weibull probability and the notch geometry. For low Weibull's modulus, survival probabilities only depend on the generalised stress intensity factor, whereas for high Weibull's modulus, probabilities also depend on the notch tip radius. The effect of the tip radius on the failure probabilities is equivalent to the exclusion of a small volume surrounding the notch tip. From these results, a numerical methodology based on the finite element analysis is proposed to state if singularity is harmful for a ceramic structure. Elsewhere, for a notch with high stress singularity order and symmetrically loaded, the Batdorf's theory gives the same results than the Weibull one. In the case of a low stress singularity order, the prediction of failure can strongly depend on the multi-axial criterion.

Keywords: Failure analysis; Structural applications; Fuel cells; Fracture; Weibull statistics

1. Introduction

Solid oxide fuel cells (SOFC) are devices allowing the conversion of chemical energy into electricity at high temperature. This type of fuel cells is mainly constituted of three ceramic layers: two porous electrodes separated by a dense electrolyte usually made of yttria-stabilised zirconia.[1] Considered as a ceramic structure, the cell presents some geometrical and material singularities where a high stress level can initiate a fracture. Ceramics and especially porous ceramics behave as brittle materials and therefore exhibit a statistical distribution on their strengths. This scattering is classically observed on brittle materials even in the case of notched specimen where the stress is localised. Indeed, some studies have been focused on the strength measurement of a series of identical ceramic single edge notched beam (SENB) specimens. Above a critical notch tip radius, the experimental toughness measurements exhibit significant scattering.[2–4] Therefore, a probabilistic approach has to be considered to describe the fracture of a notched ceramic and more generally to predict the fracture of brittle materials submitted to a singular stress field.

In this paper, it is assumed that the ceramic fracture initiated in a singular volume remains controlled by flaws contained within this zone. In this frame, the probability of fracture can be evaluated through the Weibull theory. However, this statistical approach requires an integration over the singular area that cannot be applied for high values of the Weibull's modulus and high stress singularity order.[5–7] Another difficulty comes from the multi-axial stress state which can take place in the material and requires the Batdorf approach to predict the brittle fracture.[8–10]

The aim of the paper is to establish a general methodology in order to determine numerically the survival probability of a ceramic with a singular stress field. For such purpose, a physical length scale is considered to overcome the Weibull integral divergence and the effect of stress triaxiality on failure prediction is also taken into account. The case of SOFC materials has been considered to illustrate the theoretical developments.

2. General expression of survival probabilities

2.1. Weibull approach: failure prediction in uni-axial loading

The Weibull theory[11,12] is based on two assumptions. The first one is the weakest link argument which assumes that the

* Corresponding author. Tel.: +33 4 38782210; fax: +33 4 38784139.
E-mail address: laurencin@chartreuse.cea.fr (J. Laurencin).

0955-2219/$ – see front matter © 2007 Elsevier Ltd. All rights reserved.
doi:10.1016/j.jeurceramsoc.2007.06.003

propagation of any flaw in the material leads to the total fracture of specimen. This assumption allows accounting for the volume dependence of the ceramic average strength. The second assumption concerns the shape of the distribution describing the survival probability as a function of the applied stress. This distribution function has been chosen to fit the brittle material behaviour with a good accuracy. Therefore, the Weibull theory is based on a pure statistical treatment of the experimental data. The survival probability P_s of a specimen loaded with an applied tensile stress σ is then expressed from the two previous assumptions as follows:

$$P_s(\sigma, V) = \exp\left(-\int_V \left(\frac{\sigma - \sigma_u}{\sigma_0}\right)^m \frac{dV}{V_0}\right) \quad (1)$$

where V is the volume of the specimen. The characteristic strength σ_0 represents a scale parameter for the distribution whereas the Weibull's modulus m corresponds to a shape parameter. The term V_0 is the reference volume linked to the characteristic strength. The parameter σ_u corresponds to the stress threshold below which the failure is impossible. This stress level usually tends to zero for ceramic components. The survival probability can then be described through the Weibull stress σ_w representing the stress integration over the volume:

$$P_s(\sigma, V) = \exp\left(-\left(\frac{\sigma_w}{\sigma_0}\right)^m\right)$$

$$\text{with} \quad \sigma_w = \frac{1}{V_0^{1/m}}\left\{\int_V \sigma^m \, dV\right\}^{1/m} \quad (2)$$

It is worth noting that the Weibull's modulus m is linked to the material homogeneity. If m tends to infinity, the ceramic contains a homogeneous defect distribution. It means that the failure does not present a statistical behaviour: the material strength becomes independent of the specimen volume. At the opposite side, if m is low, the strength depends strongly on the stressed volume. In this case, a small volume may withstand a high level of stress.

For a structure submitted to a multi-axial stress state, the survival probability can be expressed by the product of each survival probability in the three principal directions, providing that the three principal stresses σ_i act independently on fracture:

$$P_s(\bar{\bar{\sigma}}, V) = \prod_{i=1}^{i=3} P_s(\sigma_i, V) \quad \text{with}$$

$$P_s(\sigma_i, V) = \exp\left(-\int_V \left(\frac{\sigma_i}{\sigma_0}\right)^m \frac{dV}{V_0}\right) \quad (3)$$

This assumption is obviously unsafe because the combination of the principal stresses on a local flaw randomly oriented will induce a shear and a normal stress which will affect the failure. This limitation of the Weibull theory has been highlighted experimentally by many authors and reviewed by Lamon.[8] The statistical prediction of failure under a multi-axial stress state has been initially proposed by Batdorf and Crose[13] and then improved by several authors into a more realistic approach.[8–10]

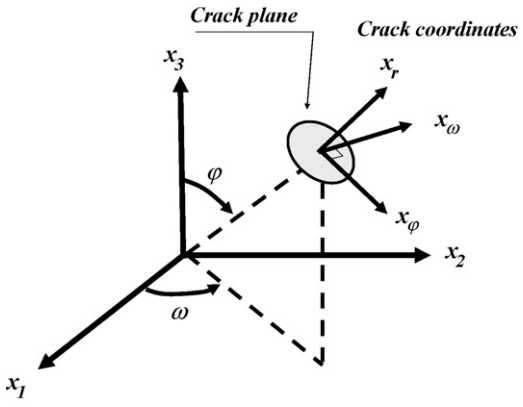

Fig. 1. Relationship between the coordinates of the principal directions (x_1 x_2 x_3) and the local coordinates related to the crack plane (x_r x_φ x_ω).

2.2. Batdorf approach: failure prediction in a multi-axial stress state

This approach considers that each natural flaw of the ceramic can be modelled by a perfect crack. These defects are submitted to a shear and normal stress due to the multi-axial loading. The local stress state (*i.e.* the mixity) depends on the location and orientation of the crack in relation to the three principal directions. According to the weakest link assumption, the failure will be reached if only one crack in the structure is submitted to an equivalent stress which exceeds a threshold value, value being determined using a crack propagation criterion. The main steps to calculate the survival probability with the Batdorf approach are the followings:

(a) Cracks are assumed to be randomly oriented in the material. The stress tensor in the local coordinate system of the defect (x_r x_φ x_ω) can be given as a function of the three principal stresses σ_1, σ_2 and σ_3 (Fig. 1):

$$\begin{bmatrix} \sigma_{rr} \\ \sigma_{r\varphi} \\ \sigma_{r\omega} \end{bmatrix} = [R] \begin{bmatrix} \sigma_1 \\ \sigma_2 \\ \sigma_3 \end{bmatrix} \quad \text{with} \quad [R] = \begin{bmatrix} \sin^2\varphi\cos^2\omega & \sin^2\varphi\sin^2\omega & \cos^2\varphi \\ \sin\varphi\cos\varphi\cos^2\omega & \sin\varphi\cos\varphi\sin^2\omega & -\sin\varphi\cos\varphi \\ -\sin\omega\cos\omega\sin\varphi & \sin\varphi\sin\omega\cos\omega & 0 \end{bmatrix} \quad (4)$$

(b) Assuming that the flaw geometry is represented by a penny-shape crack with radii c, the stress intensity factors K_I, K_{II} and K_{III} related to the three modes of loading are expressed from the local stress field surrounding the crack (Fig. 2). In the case of an infinite body, it has been demonstrated that[14]:

$$K_I = \frac{2}{\pi}\sigma\sqrt{\pi c}, \quad K_{II} = \frac{4}{\pi(2-\nu)}\tau\cos\psi\sqrt{\pi c},$$

$$K_{III} = \frac{4(1-\nu)}{\pi(2-\nu)}\tau\sin\psi\sqrt{\pi c} \quad (5a)$$

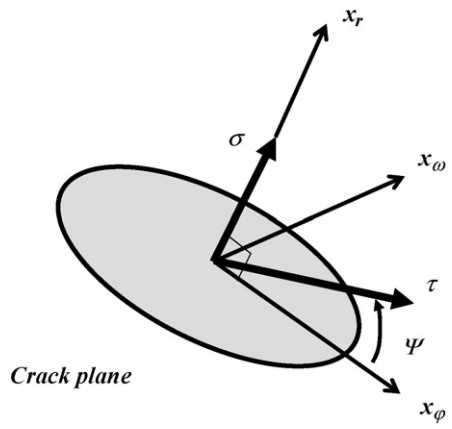

Fig. 2. Penny-shape crack loaded by a normal σ and shear τ stresses.

with

$$\sigma_{rr} = \sigma \quad \text{and} \quad \left.\begin{aligned} \sigma_{r\varphi} &= \tau \cos\psi \\ \sigma_{r\omega} &= \tau \sin\psi \end{aligned}\right\} \quad \text{with}$$

$$\tau = (\sigma_{r\varphi}^2 + \sigma_{r\omega}^2)^{1/2} \tag{5b}$$

where the symbol ν denotes the Poisson's ratio.

(c) The crack extension occurs when a combination of the stress intensity factors typically expressed as $g(K_{\mathrm{I}}, K_{\mathrm{II}}, K_{\mathrm{III}})$ exceeds a critical value g_{c} which only depends on the local toughness K_{IC}. This criterion allows defining an equivalent stress σ_{eq} which depends on local stresses (σ, τ). The failure is assumed to occur when σ_{eq} reaches a critical value related to g_{c}.

(d) The equivalent stress σ_{eq} can then be introduced in the strength distribution and integrated on the whole volume and over all angular elements (for each flaw orientation). The survival probability P_{s} is finally expressed as follows:

$$P_{\mathrm{s}} = \exp\left\{-\int_V \left(K_n \int_{\omega=0}^{\omega=\pi} \int_{\varphi=0}^{\varphi=\pi} \sigma_{\mathrm{eq}}^m \sin\varphi \,\mathrm{d}\varphi \,\mathrm{d}\omega\right) \mathrm{d}V\right\} \tag{6}$$

The coefficient K_n allows scaling the calculated probability P_{s}. The term K_n is defined in such way that the probability is reduced to the classical Weibull expression when the specimen is loaded under an homogeneous tensile stress σ_{t}:

$$K_n = \frac{1}{\pi \sigma_0^m V_0 I_m} \tag{7}$$

The term I_m is an integral which depends on the Weibull's modulus. It is worth noting that the Batdorf theory takes into account the effect of the principal stress interaction on the failure probability. Furthermore, this theory is based on physical considerations and requires the choice of a crack extension criterion.[15,16]

A multi-axial stress state can appear in the singular fields even if the sharp notch is loaded in a pure opening mode. One purpose of this paper is to estimate the influence of the singular stress field triaxiality on failure probability by using a Batdorf approach. Three classical criteria for crack extension will be investigated. The Eqs. (8)–(10) describe the expressions of (a) the equivalent stress σ_{eq} and (b) the integral I_m related to each criterion. In this work, they have been implemented in the finite element code Cast3M[17]:

(i) The first criterion is based on a crack extension in pure mode I:

$$\sigma_{\mathrm{eq}} = \sigma \tag{8a}$$

and

$$I_m = \int_{\varphi=0}^{\varphi=\pi} \cos^{2m}\varphi \,\sin\,\varphi \,\mathrm{d}\varphi = \frac{2}{2m+1} \tag{8b}$$

(ii) For the second criterion, the crack extension occurs when the maximum energy release rate for coplanar crack propagation exceeds the material toughness:

$$\sigma_{\mathrm{eq}} = \left\{\sigma^2 + \frac{4}{(2-\nu)^2}\tau^2\right\}^{1/2} \tag{9a}$$

and

$$I_m = \int_{\varphi=0}^{\varphi=\pi} \cos^m\varphi \left\{\cos^2\varphi + \frac{4}{(2-\nu)^2}\,\sin^2\varphi\right\}^{m/2} \sin\varphi \,\mathrm{d}\varphi \tag{9b}$$

(iii) For the last criterion, the crack extension is sensitive to the maximum energy release rate for non-coplanar crack propagation:

$$\sigma_{\mathrm{eq}} = \left[\sigma^4 + \left(\frac{2}{2-\nu}\right)^4 \tau^4 + 6\left(\frac{2}{2-\nu}\right)^2 \sigma^2\tau^2\right]^{1/4} \tag{10a}$$

and

$$I_m = \int_{\varphi=0}^{\varphi=\pi} \cos^m\varphi \left\{\cos^4\varphi + \frac{16}{(2-\nu)^4}\,\sin^4\varphi + \frac{24}{(2-\nu)^2}\,\sin^2\varphi\cos^2\varphi\right\}^{m/4} \sin\varphi \,\mathrm{d}\varphi \tag{10b}$$

It is worth noting that the choice of the criterion depends on the nature of the ceramic material. For example, Thiemeier et al.[15] have demonstrated that the maximum non-coplanar energy release rate criterion allows describing the aluminium nitride fracture behaviour; whereas Brückner-Foit et al.[16] have shown that flaws in silicon nitride are only sensitive to an opening mode of loading.

3. Expression of survival probabilities in a singular stress field

This section is dedicated to the prediction of failure initiated in the singularity of a V notch. The statistical approach of fracture is employed by considering the Weibull theory. First, the survival probability is calculated assuming a perfect V notch. As limitation arises for high Weibull's modulus m, the radius of

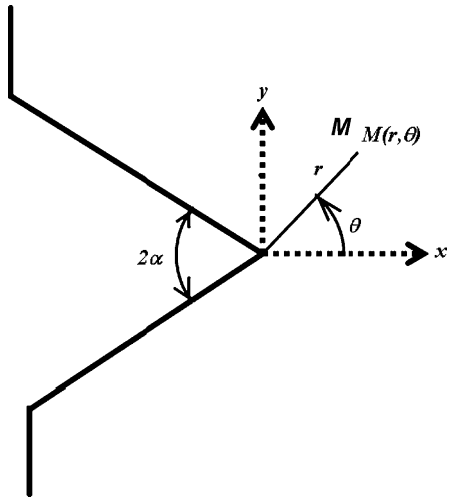

Fig. 3. Scheme of a perfect V notch in a homogeneous medium.

the notch tip is then introduced in the mathematical analysis and its influence on the survival probabilities is investigated.

3.1. Relationship between the Weibull modulus and the singularity order for a perfect V notch

Let us consider now the singular stress field created by a perfect V notch (Fig. 3). In the case of a symmetric loading, the elastic stress field is written in the vicinity of the notch tip as a function of the generalised stress intensity factor k_1 related to the opening mode. The displacements u_i and the stress tensor σ_{ij} are given by the following equations[18]:

$$u_i = k_1 r^{\lambda_1} g_i(\theta) \tag{11a}$$

$$\sigma_{ij} = k_1 r^{-\lambda_1^*} f_{ij}(\theta) \quad \text{with} \quad \lambda_1^* = 1 - \lambda_1 \tag{11b}$$

where (r,θ) is the coordinate system used for the analysis (see Fig. 3). The terms λ_1 and λ_1^* are related to the opening mode and correspond to the singularity orders, respectively, on displacements and stresses. The exponent λ_1^* decreases from 1/2 for a perfect crack (*i.e.* for a notch opening angle $2\alpha = 0$) down to 0 for a straight edge ($2\alpha = \pi$). It has been shown that the singularity orders on displacements are solutions of an eigenvalue problem.[18,19] For the symmetric field (mode I), the exponent λ_1 is given by the lowest solution of the following equation:

$$\sin\{\lambda_1(2\pi - 2\alpha)\} + \lambda_1 \sin\{2\pi - 2\alpha\} = 0 \tag{12}$$

Typical values of λ_1 and λ_1^* are tabulated in Table 1 as a function of α.

Table 1
Values of the singularity orders λ_1 and λ_1^*

2α (°)	Singularity order on displacement λ_1 (calculated from Eq. (12))	Singularity order on stress λ_1^*
90	0.5445	0.4555
120	0.6157	0.3843
140	0.6972	0.3028
150	0.7520	0.248

In order to investigate the effect of the singularity on the failure probability, the singular field (Eq. (11)) is introduced in the expression of the Weibull stress (Eq. (2)). Only the hoop stress $\sigma_{\theta\theta}$ that opens the notch has been considered for the sake of simplicity:

$$\sigma_w = \left\{ \frac{B}{V_0} \int_{\theta=-(\pi-\alpha)}^{\theta=+(\pi-\alpha)} \int_{r=0}^{r=R_k} k_1^m r^{-\lambda_1^* m} f_{\theta\theta}^m(\theta) r \, \mathrm{d}r \, \mathrm{d}\theta \right\}^{1/m} \tag{13}$$

where the integration bound R_k represents the radius of the singularity area and the term B denotes the out of plane specimen thickness.

When integrating the previous equation, it appears that Weibull stress remains finite only if $m\lambda_1^* < 2$. This condition is fulfilled when the Weibull's modulus is low enough so that the ceramic strength depends strongly on the tested volume. In this case, despite the high stress level caused by the perfect V notch tip, the volume corresponding to the singular stress field is sufficiently small to obtain a finite Weibull stress:

$$\sigma_w = \left\{ \left(\frac{B}{V_0}\right) \left(\frac{k_1^m R_k^{-\lambda_1^* m+2}}{-\lambda_1^* m + 2}\right) \int_{\theta=-(\pi-\alpha)}^{\theta=+(\pi-\alpha)} f_{\theta\theta}^m(\theta) \, \mathrm{d}\theta \right\}^{1/m}$$
$$\text{for} \quad m\lambda_1^* < 2 \tag{14}$$

If the previous condition $m\lambda_1^* < 2$ is not fulfilled, the Weibull stress is not bounded and the survival probability should tend to zero. In other words, if m is sufficiently high (volume-independent strength), the local stress would always be sufficient to induce the fracture in the singular area (whatever the level of the applied load on the notch specimen). This case is obviously unrealistic and not physically relevant.

Thus it is proposed here when $m\lambda_1^* \geq 2$ to modify the unbounded expression of the Weibull stress by introducing a length scale parameter physically meaningful.[7,20] Up to here, the studied V notch has been considered ideal. In reality, there is always a small radius at the notch tip which blunts the sharp corner (Fig. 4). This radius comes from the machining or manufacturing process and is related to the microstructure. The

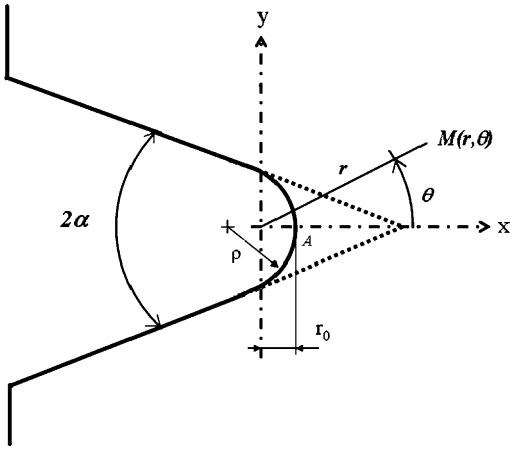

Fig. 4. Scheme of a rounded V notch in a homogeneous medium.

stress field induced by such as rounded V notch approaches closely the field of the corresponding ideal sharp V notch but remains finite at the notch tip. Therefore, the introduction of a tip radius should remove the Weibull stress singularity in the case of $m\lambda_1^* \geq 2$.

An alternative strategy consists in excluding a small volume surrounding the ideal notch tip from the domain of stress field integration arguing that ceramic defects present a minimal size. In other words, the stressed volume used for the statistical calculations has to be large enough to contain critical flaws.

The effect of introducing a notch tip radius on the survival probabilities will be first studied in the next section. Then, the approach which consists in excluding a small volume of material will be also evaluated. Finally, the consistencies between the two strategies will be assessed.

3.2. Influence of the notch tip radius on the survival probability

Filippi et al.[21] have established the analytical elastic stress field expressions in the neighbourhood of a notch with a small tip radius ρ (Fig. 4). To obtain this more accurate solution, they have added a new exponent μ to the singularity order. In the opening mode, the stress components are always linked to the stress intensity factor k_1:

$$\sigma_{\theta\theta}=k_1 r^{\lambda_1-1}\left\{f_{\theta\theta}(\lambda_1,\theta)+\frac{q}{4(q-1)}\left(\frac{r}{r_0}\right)^{\mu_1-\lambda_1} g_{\theta\theta}(\mu_1,\lambda_1,\theta)\right\} \quad (15a)$$

$$\sigma_{rr}=k_1 r^{\lambda_1-1}\left\{f_{rr}(\lambda_1,\theta)+\frac{q}{4(q-1)}\left(\frac{r}{r_0}\right)^{\mu_1-\lambda_1} g_{rr}(\mu_1,\lambda_1,\theta)\right\} \quad (15b)$$

$$\sigma_{r\theta}=k_1 r^{\lambda_1-1}\left\{f_{r\theta}(\lambda_1,\theta)+\frac{q}{4(q-1)}\left(\frac{r}{r_0}\right)^{\mu_1-\lambda_1} g_{r\theta}(\mu_1,\lambda_1,\theta)\right\} \quad (15c)$$

where $q=(2\pi-2\alpha)/\pi$ and $r_0=(\rho(q-1))/q$. The λ, μ, $f(\lambda,\theta)$ and $g(\mu,\lambda,\theta)$ terms are given in Ref. 21. The definitions of r and θ are given in Fig. 4 (with $r>r_0$ for $\theta=0$). It is worth noting that the radius perturbs the stress field only at the immediate vicinity of the notch tip. Atzori et al.[22] have demonstrated that this zone spreads over a distance of 0.4ρ from the tip. Outside this region, the stress field matches the singular one. Fig. 5 illustrates this remark. The analytical hoop stress calculated by Filippi et al. (Eq. (15a)) has been compared to the result of the finite element analysis performed in this work. The $\sigma_{\theta\theta}$ stress component has been plotted in logarithmic coordinates as a function of the distance along x from the notch tip (point A in Fig. 4). At some distance from the tip, the curve exhibits a linear evolution with a slope corresponding to the notch singularity order λ_1^*. This linear portion defines the area where the field is dominated by the singular solution described by (Eq. (11)).

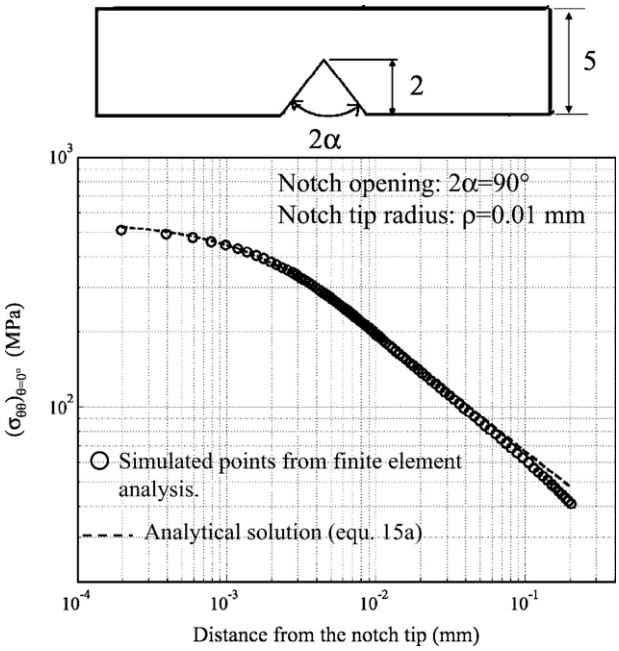

Fig. 5. Hoop stress plotted along the notch bisector ($\theta=0°$). Agreement between the analytical solution from Filippi et al.[21] and the simulated points from a finite element analysis with: $2\alpha=90°$, $\lambda_1=0.5445$, $\mu_1=0.3449$, $\rho=0.01$ mm, $k_1=2.456\,\text{MPa m}^{(1-\lambda_1)}$, $\rho=0.01$ mm (present study).

The analytical stress field (Eq. (15)) has been used to calculate the principal stresses close to the rounded V notch:

$$\sigma_{1,2}=\frac{\sigma_{\theta\theta}+\sigma_{rr}}{2}\pm\sqrt{(\sigma_{\theta\theta}-\sigma_{rr})^2+\sigma_{r\theta}^2} \quad (16a)$$

$$\sigma_3=\nu(\sigma_1+\sigma_2) \quad \text{(plane strain)} \quad (16b)$$

Then, the three principal stresses have been introduced in the Weibull distribution (Eq. (3)) and the effect of the notch tip radius on the survival probability has been investigated. The probability calculation has required a numerical integration. Fig. 6 shows the results obtained for a crack ($\alpha=0$ and $\lambda_1^*=0.5$) with a blunted tip.

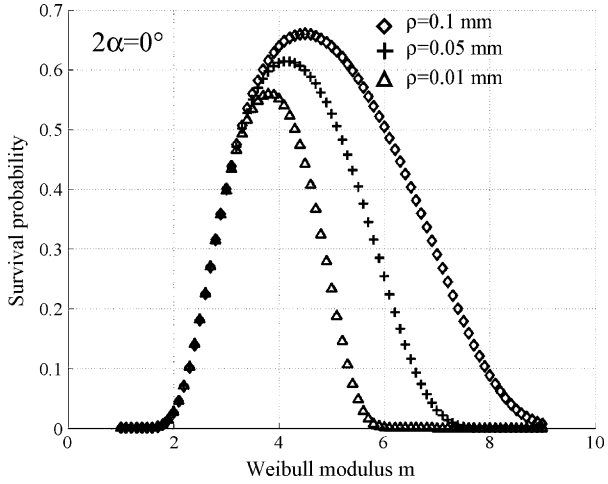

Fig. 6. Survival probability in the neighbourhood of a crack plotted as a function of the Weibull's modulus m. Three notch tip radii have been investigated: $\rho=0.01$, 0.05 and 0.1 mm ($2\alpha=0°$, $\lambda_1=0.5$, $k_1=0.316\,\text{MPa}\sqrt{\text{m}}$, $\sigma_0=12.5$ MPa, $V_0=1\,\text{mm}^3$).

In the case of $m\lambda_1^* \geq 2$ (*i.e.* $m \geq 4$ for a crack), the survival probability is found to present non-zero values for the three studied notch tip radii ($\rho = 0.01$, 0.05 and 0.1 mm). As foreseen, this result indicates that the divergence on the Weibull stress has been removed. The survival probability P_s varies with the notch radius: P_s decreases strongly when ρ is decreased. Indeed, since the Weibull modulus considered in this case is high, the probability calculation is mainly sensitive to the volume perturbed by the notch tip. In other words, the risk of rupture is localised and controlled by this perturbed volume. If the tip radius tends to zero, P_s also tends to zero because the Weibull stress integration becomes unbounded ($P_s \to 0$).

In the case of $m\lambda_1^* < 2$ (*i.e.* $m < 4$ for a crack), the survival probabilities are found to be almost independent of the notch tip radius and its value is similar to that determined with the expression of the singular field (Eq. (11)). Indeed, in this case, the Weibull stress is not affected by the small volume in the vicinity of the rounded notch tip. As a consequence, the risk of rupture spreads beyond this high stressed zone.

3.3. Expression of the survival probability for $m\lambda_1^* \geq 2$

The aim of this section is to express in the case of $m\lambda_1^* \geq 2$ the survival probability as a function of:

- the notch tip radius (case of a blunted notch).
- the size of the excluded zone (case of an ideal sharp notch).

The equivalence between the two approaches has been also established.

3.3.1. Case of a blunted notch

As shown in the previous section, the Weibull probability depends strongly on the notch tip radius. To determine the analytical relationship between P_s and ρ, the stress field established close to the notch tip (Eq. (15)) has been introduced into the Weibull distribution (Eq. (1)). The calculation detailed in Appendix A leads to:

$$\ln P_s = -\left[\frac{k_1}{k_0(\rho)}\right]^m \quad \text{with} \quad k_0(\rho) = \sigma_0 \left[\frac{V_0}{B\Omega_\theta}\right]^{1/m} \rho^{(m\lambda_1^* - 2)/m} \tag{17}$$

The dimensionless term Ω_θ depends on the Weibull's modulus, the notch opening angle α and the exponents λ_1 and μ_1. The term $k_0(\rho)$ can be interpreted as a characteristic toughness of the notched specimens which leads to a survival probability of 0.37 when the generalised stress intensity factor reaches this value $k_1 = k_0$. For $m \to \infty$ (*i.e.* the strength is not probabilistic), it can be highlighted that the toughness reduces to the form of $k_0(\rho) \propto \sigma_0 \rho^{\lambda_1^*}$ which is identical to a rupture stress criterion.

To verify the relationship between the notch tip radius and the survival probability, a finite element analysis has been performed for a 90° notch opening angle. The simulations have been carried out for various tip radii ranging from 0.01 to 0.1 mm. The evolution of the survival probability with the notch radius obtained by the finite element analysis is perfectly described by a law under the form: $\ln P_s \propto \rho^{-m\lambda_1^* + 2}$ (Fig. 7). This last result proves the accuracy of the Eq. (17) which establishes the dependence of the survival probability with the notch tip radius.

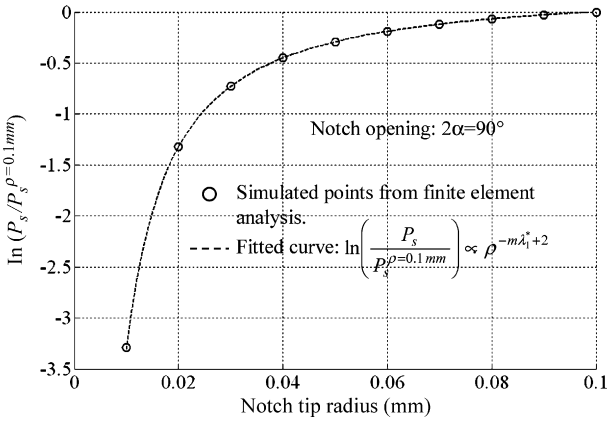

Fig. 7. Logarithm of the normalised survival probability $P_s/P_s^{\rho=0.1\,\text{mm}}$ plotted as a function of the notch tip radius. The simulated points have been fitted by Eq. (17) ($2\alpha = 90°$, $\lambda_1 = 0.5445$, $m = 7$).

3.3.2. Case of a sharp V notch with an excluded zone

The survival probability can also be determined by using the expression of the singular stress field of a sharp V notch and removing from the singular area a small region surrounding the notch tip. If r_c denotes the characteristic radius of this zone, it will be defined in such way that the Weibull stress calculated from the singular field into the annular region $r_c < r < R_k$ is equivalent to the one determined in the presence of a notch tip radius (Fig. 8).

The survival probability P_s calculated by using the singular field integrated into the area defined by $r_c < r < R_k$ is given by (see Appendix B):

$$\ln P_s = -\left[\frac{k_1}{k_0'(r_c)}\right]^m \quad \text{with} \quad k_0'(r_c) = \sigma_0 \left[\frac{V_0}{B\Lambda_\theta}\right]^{1/m} r_c^{(m\lambda_1^* - 2)/m} \tag{18}$$

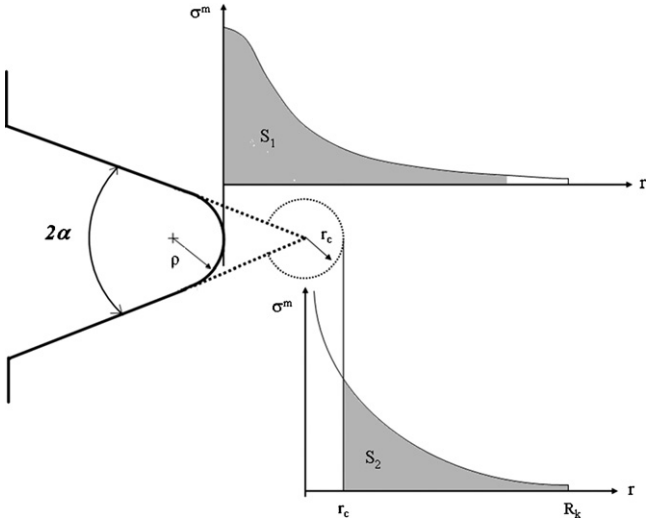

Fig. 8. Definition of the characteristic radius r_c: the Weibull stress S_2 calculated from the singular field into the annular region $r_c < r < R_k$ must be equal to the one determined in the presence of a notch tip radius S_1.

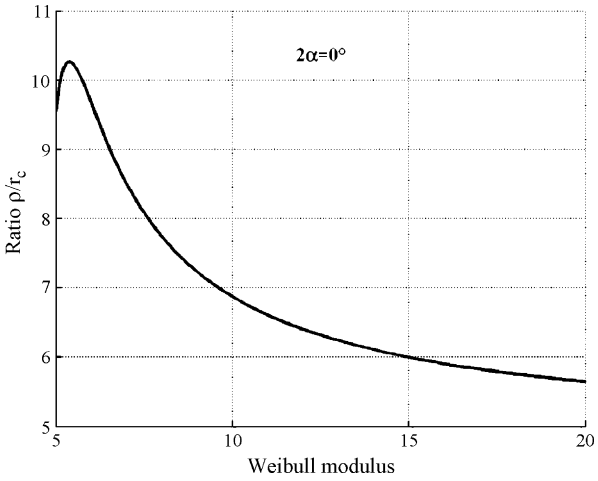

Fig. 9. Ratio of the notch tip radius ρ over the characteristic radius r_c plotted for a crack as a function of the Weibull's modulus.

where Λ_θ depends on the notch opening α and the singularity order λ_1. The relationship between the characteristic radius r_c and the notch tip radius can be inferred from Eqs. (17) and (18):

$$\frac{\rho}{r_c} = \left(\frac{\Omega_\theta(m, \alpha, \lambda_1^*, \mu_1)}{\Lambda_\theta(m, \alpha, \lambda_1^*)} \right)^{1/(m\lambda_1^* - 2)} \tag{19}$$

The last equation shows that there is a linear dependence between the characteristic radius r_c and the notch tip radius ρ with a slope depending only on the Weibull's modulus and notch opening. The ratio ρ/r_c has been plotted as a function of the Weibull modulus in the case of a crack (Fig. 9). The terms Ω_θ and Λ_θ have been calculated in plane deformation by taking into account the three principal stresses. It can be noticed that for materials having a Weibull's modulus ranging from 5 to 7, the ratio is about 10.

The equivalence between ρ and r_c will be used into a numerical methodology to state if a singularity is harmful (see Section 5.1).

4. Finite element analysis of survival probability calculated at singularity

4.1. Introduction: conditions of the simulations

In order to illustrate the results presented in the previous section, a finite element analysis has been carried out to study the failure probability of a notched beam. The specimen has been simulated in a four-point flexural test bench in such a way that the notch is submitted to an opening mode of loading. The dimensions of the specimen are specified in Fig. 10. The spacing of the outer bearings is fixed to 40 mm whereas the spacing of the inner ones is 20 mm.The material characteristics considered for this study are given in Table 2. They are representative of 8YSZ (8 mol% yttria stabilised zirconia) which is a classical SOFC electrolyte material.[23,24] Four notch opening angles with an ideal V shape ($\rho = 0$) have been simulated ($2\alpha = 90$, 120, 140 and 150°). The effect of the notch tip radius has also been studied. Three radii ($\rho = 0.01$, 0.05 and 0.1 mm) have been investigated on specimens for which the V notch geometry implies that the criterion $m\lambda_1^* \geq 2$ is verified (*i.e.* for $2\alpha = 90$ and 120° as calculated in Table 3).

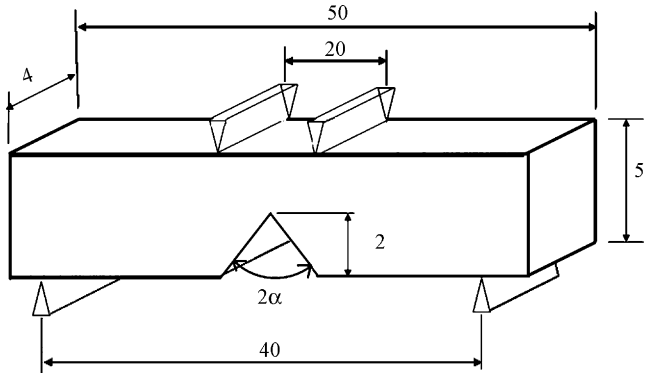

Fig. 10. Scheme of the simulated flexural test. Lengths are given in millimeters. Simulations are performed by blocking the outer bearings and applying an imposed displacement to inner ones.

Table 2
Material characteristics: elastic coefficients and Weibull parameters

Young modulus, E (GPa)	Poisson's ratio, ν	Weibull's modulus, m	Characteristic strength, σ_0 (MPa)	Characteristic volume, V_0 (mm^3)
190[23]	0.308[23]	7[24]	446[24]	102

To study the influence of the singular stress triaxiality on the failure probability, the Batdorf's approach has been applied on the notched specimens. The three classical criteria presented in Section 2.2 have been investigated and implemented in the finite element code. It is reminded that the criteria considered in this paper are based on (i) a mode I failure, (ii) the maximum coplanar energy release rate and (iii) the maximum non-coplanar energy release rate. In a first approach, it has been assumed that the stress intensity factors established for an infinite body (Eq. (5)) remains relevant for defects close to the notch tip. Taking into account stress triaxiality on the failure probability requires integrating some trigonometric functions over all angular elements (Eqs. (8b), (9b) and (10b)). For the mode I criterion, this integral exhibits an analytical solution. However, the two other criteria, the integral I_m has to be numerically computed. A special attention has been paid to choose a sufficiently small angular element to integrate the trigonometric functions with accuracy.

The model used to perform the finite element simulations is based on an elastic behaviour of the ceramic specimen. A fine mesh at the tip of the sharp and blunted V notch has been made to compute accurately the divergence of the stress field

Table 3
Values of the singularity exponent and $m\lambda_1^*$ product

2α (°)	$\lambda_1^* = 1 - \lambda_1$	$m\lambda_1^*$
90	0.4555	3.1885
120	0.3843	2.6901
140	0.3028	2.1196
150	0.248	1.736

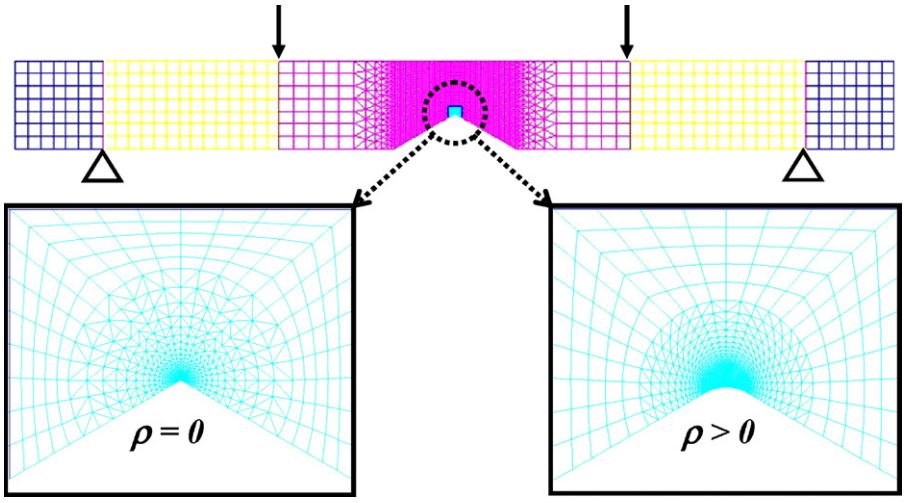

Fig. 11. Mesh of the flexural specimen. Arrangement of elements at the notch tip (for an ideal V notch and a blunted one).

(Fig. 11). Eight-node 2-D elements have been used to design the mesh and the computations have been performed considering the plane strain assumption. The finite element code Cast3m[17] has been employed for the analysis.

4.2. Results

4.2.1. Weibull probabilities for a sharp V notch

The V notch induces a stress singularity as it is observed in Fig. 12 where the logarithm of the hoop stress as been plotted along the bisector (for $2\alpha = 120^\circ$). The linear part of the curve defines the k-dominance radius R_k in which the fields are governed by the singularity (Eq. (11)). It can be noticed that R_k is found to be equal to around 0.2 mm which corresponds to one-tenth of the notch length. According to Eq. (11), the slope of the curve plotted in Fig. 12 gives the singularity order λ_1^* which is estimated to be 0.3853. This last value is in good agreement with the singularity exponent obtained from Eq. (12) (see Table 1). This result proves the accuracy of the singular stress field determined by the finite element analysis.

As discussed in Section 3.1, the Weibull stress diverges to infinity when the term $m\lambda_1^*$ is higher than 2. This result must lead to a mesh dependence of the survival probability P_s calculated from the finite element stress solution. In the case of a 90° notch opening, the survival probability has been plotted as a function of the applied displacement for various mesh densities, *i.e.* for various sizes R_{min} of the notch tip elements (Fig. 13). As foreseen, the survival probability predicted from the finite element analysis decreases when the mesh size is decreased.

In Fig. 14, the survival probabilities have been divided by a chosen reference value $P_{s,max}$ fixed to 0.42. For each notch opening angle, the applied displacements have been adjusted to obtain this $P_{s,max} = 0.42$ for the coarser mesh size. This normalised probability $P_s/(P_{s,max} = 0.42)$ has then been plotted as a function of R_{min} for the investigated notch openings (Fig. 14). It can be observed than when $m\lambda_1^*$ is higher than 2, the probability is mesh dependent. However, this dependence vanishes as soon as the term $m\lambda_1^*$ becomes lower than 2. As expected, this result illustrates the special role of the limiting value $m\lambda_1^* = 2$ on the probability fracture behaviour of a notched specimen.

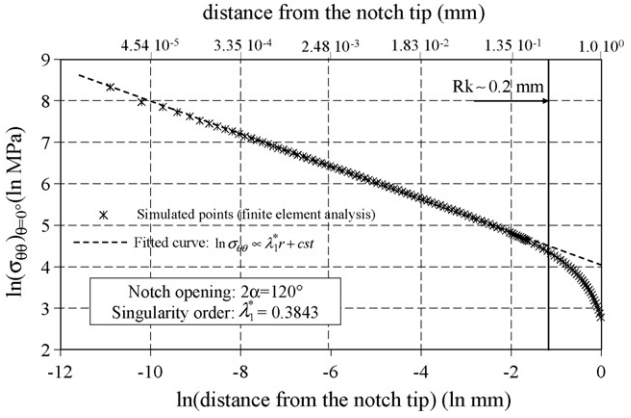

Fig. 12. The logarithm of the $\sigma_{\theta\theta}$ stress component has been plotted as a function of the distance from the notch tip (along the bisector: $\theta = 0^\circ$ and for the notch opening: $2\alpha = 120^\circ$).

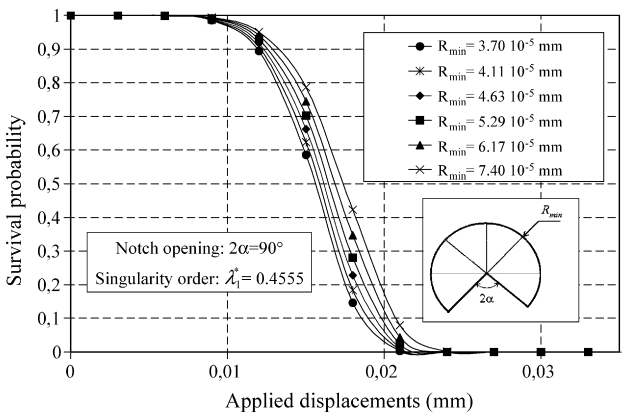

Fig. 13. Survival probability P_s plotted as a function of the applied displacements. P_s has been obtained for different mesh sizes (R_{min} is the radius of the notch tip elements, $m = 7$).

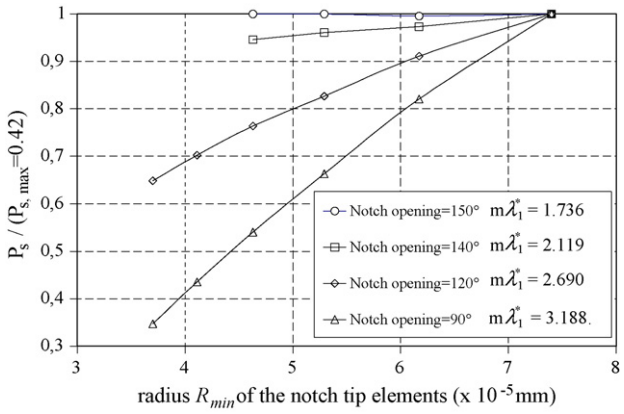

Fig. 14. Normalised survival probability plotted as a function of the radius of the notch tip elements. The mesh size dependence on P_s has been investigated for different notch opening angles.

4.2.2. Weibull probabilities for a blunted V notch

In the case of $m\lambda_1^* \geq 2$, the effect of a notch tip radius has been investigated. For a 90° notch opening, the survival probabilities obtained respectively for a tip radius of $\rho = 0.1$ and 0.01 mm have been compared to those calculated from the sharp V notch (Fig. 15). To achieve a good match between the two curves, a small region surrounding the tip of the sharp V notch has been removed from the singular area. The characteristic radius of this excluded zone r_c is found to be approximately 10 times smaller than the notch tip radius. The extent of the region removed remains much smaller than the k-dominance area. Indeed, R_k is equal to around 0.2 mm whereas the characteristic radius r_c varies over a range from 10^{-3} to 10^{-4} mm. These results coming from the finite element analysis are consistent with the theoretical analysis presented in Section 3.3.

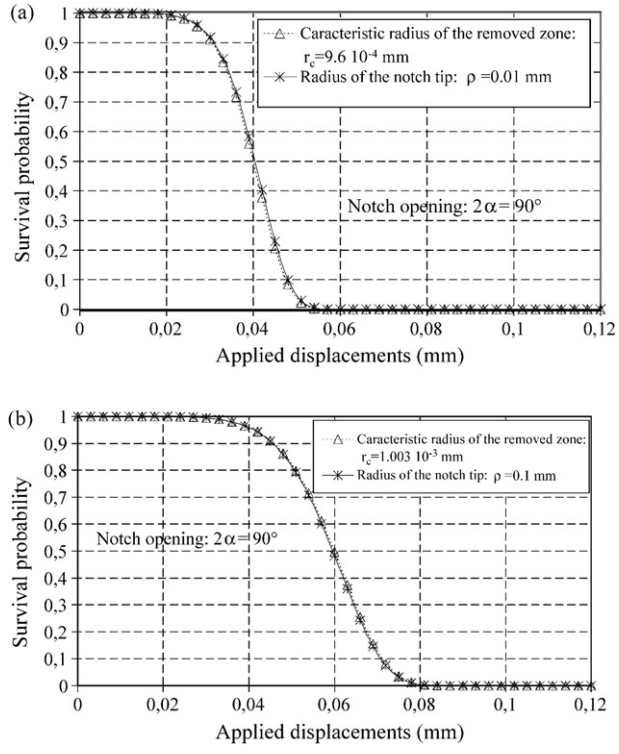

Fig. 15. Survival probability P_s plotted as a function of the applied displacements ($2\alpha = 90°$). The probabilities have been calculated for (i) a rounded V notch and (ii) a sharp V notch with a small region removed in the vicinity of the singularity: (a) notch tip radius $\rho = 0.01$ mm; (b) notch tip radius $\rho = 0.1$ mm.

4.2.3. Survival probability calculated with the Batdorf approach

Fig. 16 shows a comparison between the survival probabilities calculated from the Weibull (according to Eq. (3)) and the Batdorf approach. For the 120° and 90° notch opening angle

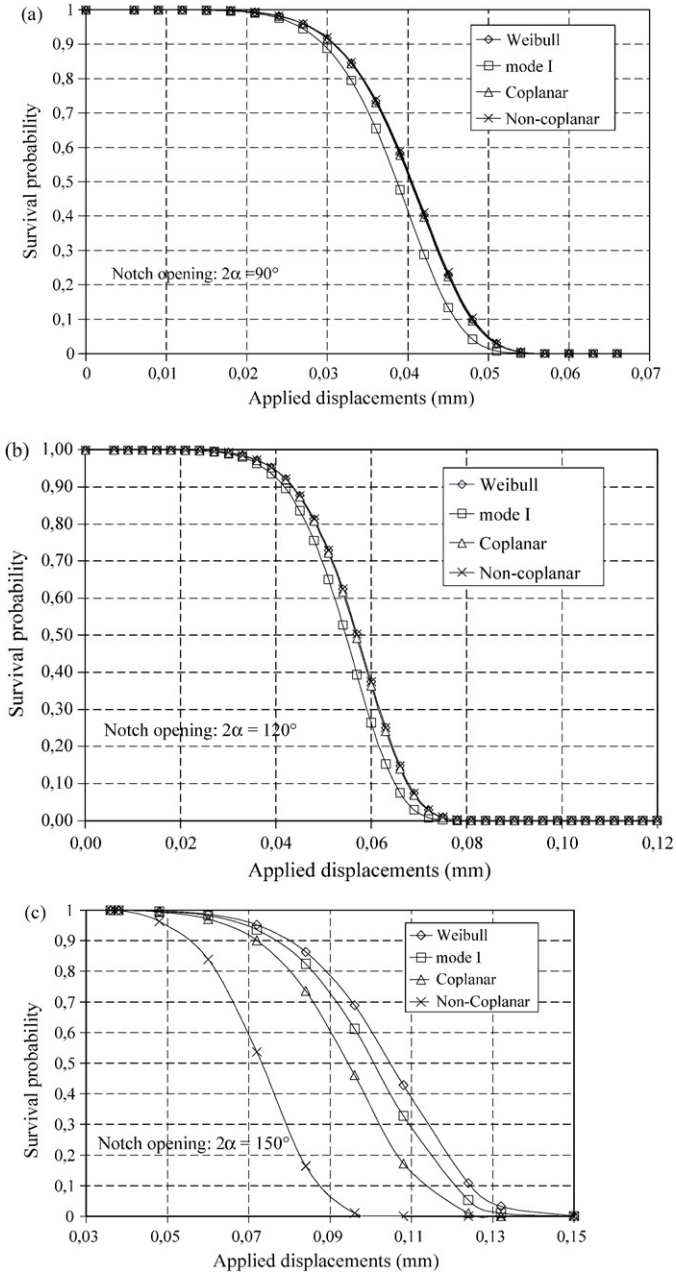

Fig. 16. Survival probability P_s plotted as a function the applied displacements for three notch opening angles. Comparison between the probabilities calculated from the Weibull and Batdorf theories: (a) notch opening angle $2\alpha = 90°$ ($\rho = 0.01$ mm); (b) notch opening angle $2\alpha = 120°$ ($\rho = 0.01$ mm); (c) notch opening angle $2\alpha = 150°$ (without notch tip radius).

(Fig. 16a and b), the survival probabilities are very close to each other. If the notch opening is increased to 150° (Fig. 16c), a strong discrepancy between the results arises. In this case, the choice of local crack extension criterion affects strongly the calculated survival probabilities.

5. Discussion

5.1. Effect of the singular stress field on ceramic failure

5.1.1. Comparison of the failure prediction with experimental trends

It has been shown in Section 3 that the failure probability of a notched structure is independent of the notch tip geometry when the condition $m\lambda_1^* < 2$ is fulfilled. Practically, this corresponds to low stress order exponent of singularities such as notches with large opening angles ($2\alpha > 150°$ for SOFC materials). For these configurations, the statistical approach developed for brittle materials applies, despite the singular stress field. The contribution to the Weibull stress of the zone around the notch (*i.e.* the singular area delimited by a distance R_k from the tip) is bounded according to the Eq. (14). As a consequence, the numerical calculation of the failure risk applied on the whole structure is not dependent of the singularity mesh size in a finite element analysis.

The extension of the Weibull analysis to lower opening angles (*i.e*. higher stress singularity orders) remains possible for rounded-tip notches. It is found that the failure is completely driven by the notch area and remains intrinsically statistical.

It is interesting to note that, for cracks ($\lambda_1^* = 0.5$), the characteristic toughness k_0 derived in Section 3.3 increases according to a law close to the square root of the tip radius. This result is consistent with the usual trend observed during the calibration of the toughness measurement on SENB specimens. Indeed, it has been widely reported that the toughness of ceramic materials evolves with the square root of the tip radius when this radius exceed a critical value ρ_c.[2,25] Moreover, for $\rho > \rho_c$, the material toughness determined for a given notch tip radius exhibits a statistical scattering. Thus, the Weibull approach seems to be well adapted to describe the failure when the notch tip radius exceeds the critical value ρ_c, typically of the order of 10 μm.[25]

5.1.2. Relation with the classical criteria of fracture mechanics

In the particular case of a blunted shaped macroscopic crack ($2\alpha = 0°$ and $\rho > 0$) placed in a homogeneous material ($m \to \infty$), the Weibull analysis deduced from Eq. (17) predicts the rupture to occur when the following condition is fulfilled:

$$\sigma_\infty \geq \beta\sigma_0 \left[\frac{\rho}{a}\right]^{0,5} \tag{20}$$

where σ_∞ is the load applied on the specimen, β a constant depending on the geometry and a is the macroscopic crack length. This condition corresponds to a stress-based criterion for failure.

Above the critical notch tip radius ρ_c, this stress criterion is equivalent to the classical approach taking into account the stress concentration factor at the tip of a rounded notch.[26]

On the contrary, for $\rho < \rho_c$, the toughness becomes independent of ρ and is considered as the true material toughness by experimenters.[2,25] In this case, the fracture mechanism is governed by the extension of the macroscopic crack and is better described by the Griffith theory based on an energy criterion.[27] The Weibull analysis fails to catch this behaviour for $\rho < \rho_c$ because it cannot describe the extension of the macroscopic crack itself.

5.1.3. Application to a brittle structure such as SOFC

The macroscopic crack extension mode is dominant in SOFC ceramic materials only for sharp cracks (with notch radius lower than 10–20 μm). Other singularities result from the cell structure and are typically 90° shaped edges. The geometries of the notch tips are expected to be rounded or blunted due to the cell elaboration process. In these conditions, the statistical approach proposed in this work is well appropriate to evaluate the impact of the singularities on the cell integrity.

In the frame of a finite element analysis, a methodology is proposed to evaluate the singularities of the structure. For each singularity, the procedure is the following:

(i) The real notch is simply meshed considering an ideal shape without describing the notch tip radius.
(ii) The finite element computation is performed and the stress field is extracted, then integrated on each element to determine the failure probability.
(iii) The failure probability is computed again after removing from the domain of integration the first rings of elements surrounding the tip and contained in the *k*-dominance zone.

Two cases can arise:

- If the failure probability is not dependent on the excluded zone surrounding the notch tip, it means that the singularity order and the Weibull's modulus are such that the probability is not sensitive to the radius of the notch tip. Therefore, the calculated failure probability can be directly calculated on the mesh of the whole ceramic component without excluding any volume surrounding the singularity. In this case, the singularity is harmless.
- If the failure probability is sensitive to the excluded zone, it means that the ceramic fracture is dependent on the notch tip radius. In this case, the failure probability has to be evaluated by excluding a zone from the tip, the radius of this zone being linked to the real notch tip radius (Eq. (19)). In this case, the singularity is clearly harmful.

5.2. Batdorf approach applied at singularity

Under a pure symmetrical mode of loading (mode I), the probability calculated from the Batdorf theory has been shown to reduce to the Weibull one when the notch angle is sufficiently small (below $2\alpha = 120°$; Fig. 16). To explain this result, the

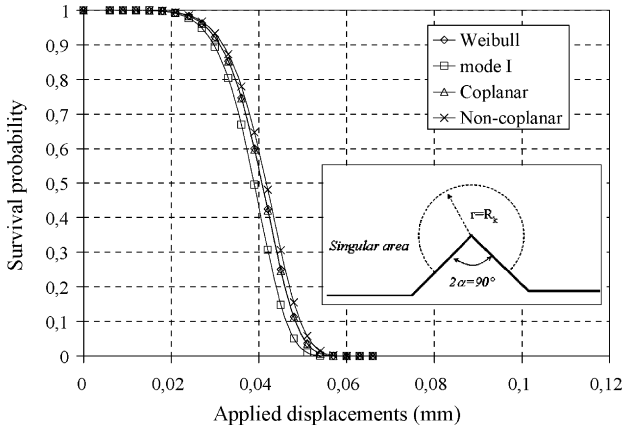

Fig. 17. The survival probability P_s has been calculated over the singular area ($R_k = 0.2$ mm) and plotted as a function the applied displacements ($2\alpha = 90^\circ$ and $\rho = 0.01$ mm).

Weibull and Batdorf survival probabilities have been calculated again but considering only the cross section of the singular zone (*i.e.* the circular region surrounding the notch tip defined by the radius $R_k \sim 0.2$ mm).

Fig. 17 illustrates the results obtained at low notch opening angle ($2\alpha = 90^\circ$). A comparison between the probabilities calculated on the singular area and the probabilities calculated on the whole specimen are given on Fig. 18 for an applied displacement of 0.039 mm. It can be noticed that, for Weibull and each criterion of the Batdorf approach (*i.e.* mode I, coplanar and non-coplanar), the survival probabilities calculated on the singular area are close to the one calculated on the whole specimen. Therefore, for both approaches, the risk of rupture of the whole structure is localised inside the singularity. In this region, the principal stress σ_1 perpendicular to the notch bisector is in traction and is much higher than σ_2. In this condition, the probabilities calculated from the Batdorf approach will necessarily match with the Weibull ones.

At the notch opening angle $2\alpha = 150^\circ$, the Batdorf and Weibull approaches were found to lead to different predictions (Fig. 16c). Fig. 19 shows the survival probabilities calculated on the singular area. The comparison with the probability computed on the whole specimen is given on Fig. 20. It can be noticed

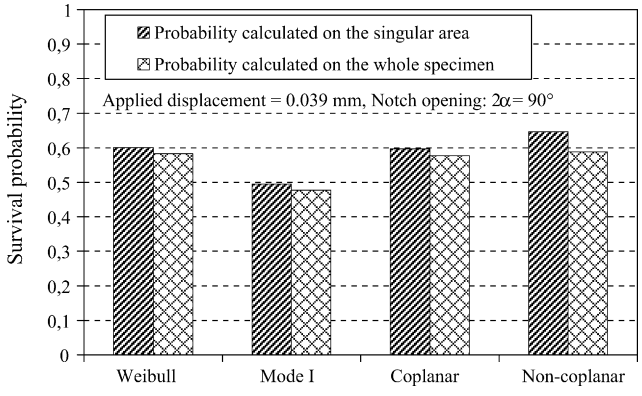

Fig. 18. Comparison between the probabilities calculated on the whole specimen and on the singular area (applied displacement = 0.039 mm, $2\alpha = 90^\circ$ and $\rho = 0.01$ mm).

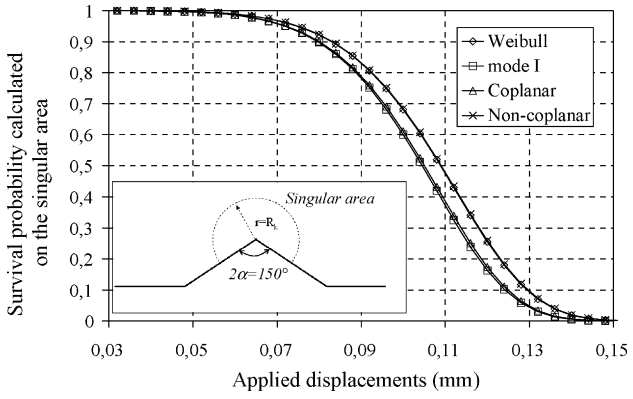

Fig. 19. The survival probability P_s has been calculated over the singular area ($R_k = 0.2$ mm) and plotted as a function the applied displacements ($2\alpha = 150^\circ$).

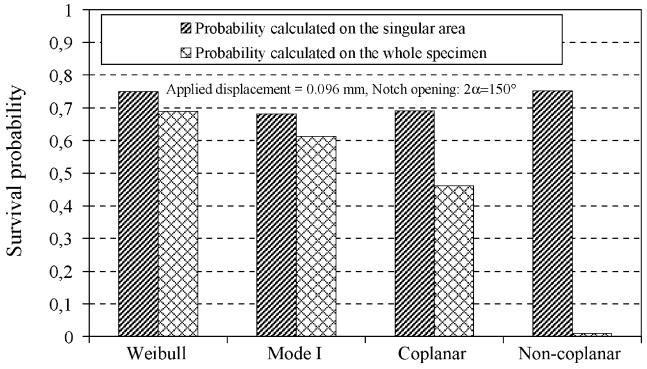

Fig. 20. Comparison between the probabilities calculated on the whole specimen and on the singular area (applied displacement = 0.096 mm, $2\alpha = 90^\circ$ and $\rho = 0.01$ mm).

that the Weibull predictions computed on the singular area are close to the probabilities calculated on the whole specimen. Furthermore, the probabilities determined from the Batdorf theory and calculated on the singular area reduced to the Weibull ones. Consequently, for the three criteria of the Batdorf approach, the region in which the local risk of fracture is high spreads beyond the *k*-dominance area; whereas, for the Weibull theory, the risk of rupture remains localised inside the vicinity of the notch tip. This result demonstrates that the differences which arise with the Batdorf survival probabilities calculated on the whole specimen are caused by the contribution of probabilities calculated on region beyond the singular area.

From this part, it can be concluded that, under a pure opening mode of loading and for a low notch opening angles, the criteria of the Batdorf theory give the same prediction than the Weibull probability. Therefore, the Weibull theory can be directly applied to calculate the risk of failure of blunted notched specimen symmetrically loaded. This conclusion remains valid as long as the notch opening angle is sufficiently small. Otherwise, the Batdorf approach has to be considered.

6. Conclusion

The limitations of the statistical approach to predict the failure of brittle specimen containing ideal V notch have been

highlighted. To overcome these difficulties, the effect of the notch tip radius ρ has been investigated. The explicit expressions of stress field ahead a rounded notch have been introduced in the Weibull analysis. It has been shown that for a low stress singularity order ($\lambda_1^* \to 0$ or $2\alpha \to 180^\circ$) and a low Weibull's modulus, the survival probabilities P_s only depend on the generalised stress intensity factor k_1 (*i.e.* the remote applied loading and the geometry of the structure). At the opposite, for a high singularity order ($\lambda_1^* \to 1/2$ or $2\alpha \to 0^\circ$) and a high Weibull's modulus, the survival probabilities depend not only on the k_1 parameter but also on the notch tip radius ρ. The explicit relationship between P_s and ρ has been established and found to be consistent with experimental trends. It has been demonstrated that the effect of the notch tip radius on the failure probabilities is equivalent to exclude a small area surrounding the tip of the ideal V notch. From these previous analyses, a numerical methodology based on the finite element method has been proposed to state the singularity harmfulness of a structure and then compute its failure probability.

The effect of the more realist Batdorf approach to predict the failure probability of the singularities has been also studied. It has been shown that under a pure symmetrical mode of loading (mode I) and a high singularity order ($\lambda_1^* \to 1/2$ or $2\alpha \to 0^\circ$), the classical criteria of defects extension implemented in the Batdorf theory give the same results than the Weibull one. However, in the case of a low singularity order ($\lambda_1^* \to 0$ or $2\alpha \to 180^\circ$), it has been also shown that the prediction of failure can strongly depend on the multi-axial criteria.

Acknowledgments

The authors warmly acknowledge Dr. Leguillon and Dr. Lefebvre-Joud for their advises and numerous helpful discussions. A part of this work has been obtained in the framework of CIEL, a research program financed by the French ANR agency and managed by Mr. S. Hody from Gaz de France (contract number ANR-05-PanH-024).

Appendix A. Relationship between the notch tip radius and the survival probability for $m\lambda_1^* > 2$

For simplifications, only the hoop stress has been taken into account in the following analysis:

$$\sigma_{\theta\theta}=k_1 r^{\lambda_1-1}\left\{f_{\theta\theta}(\lambda_1,\theta)+\frac{q}{4(q-1)}\left(\frac{r}{r_0}\right)^{\mu_1-\lambda_1} g_{\theta\theta}(\mu_1,\lambda_1,\theta)\right\} \tag{A1.1}$$

with $q=(2\pi-2\alpha)/\pi$ and $r_0=(\rho(q-1))/q$. The previous stress component is introduced in the Weibull distribution. The survival probability calculation leads to a stress integral J defined as:

$$P_s = \exp\left(-\frac{J}{{\sigma_0}^m V_0}\right) \quad \text{with}$$

$$J = B\int_{\theta=-(\pi-\alpha)}^{\theta=+(\pi-\alpha)}\int_{r=r_0}^{r=R_k} k_1^m f_{\theta\theta}^m(\lambda_1,\theta) \times\left\{r^{\lambda_1-1}+\frac{q}{4(q-1)}\frac{r^{\mu_1-1}}{r_0^{\mu_1-\lambda_1}}\frac{g_{\theta\theta}(\mu_1,\lambda_1,\theta)}{f_{\theta\theta}(\lambda_1,\theta)}\right\}^m r\,\mathrm{d}r\,\mathrm{d}\theta \tag{A1.2}$$

where B denotes the specimen thickness. The function can be developed before integration:

$$J = B\int_{\theta=-(\pi-\alpha)}^{\theta=+(\pi-\alpha)}\int_{r=r_0}^{r=R_k} k_1^m f_{\theta\theta}^m\left\{\sum_{p=0}^{p=m}\frac{m!}{p!(m-p)!}\left(\frac{q}{4(q-1)}\frac{g_{\theta\theta}}{f_{\theta\theta}}\right)^{m-p}\frac{r^{p(\lambda_1-1)+(m-p)(\mu_1-1)+1}}{r_0^{(m-p)(\mu_1-\lambda_1)}}\right\}\mathrm{d}r\,\mathrm{d}\theta \tag{A1.3}$$

If $R_k \gg r_0$ and $p(\lambda_1-1)+(m-p)\ (\mu_1-1)+2<0$, the integration of J gives the following expression (A1.4). It can be noticed that the second condition is fulfilled when $m(\lambda_1-1)<-2$ (whatever the value of p).

$$J = Bk_1^m r_0^{m(\lambda_1-1)+2} I_\theta \quad \text{with}$$

$$I_\theta = \int_{\theta=-(\pi-\alpha)}^{\theta=+(\pi-\alpha)} f_{\theta\theta}^m \sum_{p=0}^{p=m}\frac{m!}{p!(m-p)!}\left(\frac{q}{4(q-1)}\frac{g_{\theta\theta}}{f_{\theta\theta}}\right)^{m-p} \times\frac{-1}{p(\lambda_1-1)+(m-p)(\mu_1-1)+2}\mathrm{d}\theta \tag{A1.4}$$

As $r_0=(\rho(q-1))/q$, the probability can be finally expressed as following:

$$P_s = \exp\left(-\frac{Bk_1^m \rho^{m(\lambda_1-1)+2}\Omega_\theta}{{\sigma_0}^m V_0}\right) \tag{A1.5}$$

The terms Ω_θ depend on the Weibull's modus, the notch opening α and the stress exponents λ_1 and μ_1. It must be numerically calculated:

$$\Omega_\theta = \left(\frac{q-1}{q}\right)^{m(\lambda_1-1)+2} I_\theta,$$

$$I_\theta = \int_{\theta=-(\pi-\alpha)}^{\theta=+(\pi-\alpha)} f_{\theta\theta}^m \sum_{p=0}^{p=m}\frac{m!}{p!(m-p)!}\left(\frac{q}{4(q-1)}\frac{g_{\theta\theta}}{f_{\theta\theta}}\right)^{m-p} \times\frac{-1}{p(\lambda_1-1)+(m-p)(\mu_1-1)+2}\mathrm{d}\theta \tag{A1.6}$$

Only the stress hoop $\sigma_{\theta\theta}$ has been taken into account to demonstrate the previous equation. However, it is important to underline that this assumption does not change the relation between P_s and ρ. The account of the other stress components into the principal stress will only affect the expression of Ω_θ.

The relation (A1.5) can be rewritten by using a characteristic toughness k_0 and the stress singularity order $\lambda_1^*(=1-\lambda_1)$:

$$\ln P_s = -\left[\frac{k_1}{k_0(\rho)}\right]^m \quad \text{with} \quad k_0(\rho)=\sigma_0\left[\frac{V_0}{B\Omega_\theta}\right]^{1/m}\rho^{(m\lambda_1^*-2)/m} \tag{A1.7}$$

It can be noticed that the relationship reduces to those established for crack by O'Dowd ($\lambda_1^* = 0.5$).[7]

Appendix B. Relationship between the characteristic radius r_c and the survival probability for $m\lambda_1^* > 2$

To simplify the write, only the singular hoop stress has been taken into account in the following analysis:

$$\sigma_{\theta\theta} = k_1 r^{-\lambda_1^*} f_{\theta\theta}(\theta) \tag{A2.1}$$

The survival probability is calculated onto an annular region defined by $r_c < r < R_k$:

$$P_s = \exp\left(-\frac{J}{{\sigma_0}^m V_0}\right) \quad \text{with}$$

$$J = B\int_{\theta=-(\pi-\alpha)}^{\theta=+(\pi-\alpha)}\int_{r=r_c}^{r=R_k} k_1^m r^{-m\lambda_1^*} f^m(\theta) r\,\mathrm{d}r\,\mathrm{d}\theta \tag{A2.2}$$

If r_c is sufficiently small in comparison to R_k and $m\lambda_1^* > 2$, J can be integrated:

$$J = Bk_1^m {r_c}^{-m\lambda_1^*+2} \Lambda_\theta \quad \text{with} \quad \Lambda_\theta = \int_{\theta=-(\pi-\alpha)}^{\theta=+(\pi-\alpha)} \frac{-f_{\theta\theta}^m(\theta)}{-m\lambda_1^*+2}\mathrm{d}\theta \tag{A2.3}$$

The term Λ_θ depends on the Weibull modulus, the notch opening α and the stress order λ_1^*. The survival probability can be finally expressed as following:

$$P_s = \exp\left(-\frac{Bk_1^m {r_c}^{-m\lambda_1^*+2}\Lambda_\theta}{{\sigma_0}^m V_0}\right) \tag{A2.4}$$

This last expression has been obtained by considering the singular hoop stress component. For a more accurate solution, the three principal stresses must be introduced in the Weibull expression. However, it is important to underline that this correction will only affect the term $\Lambda_\theta(m,\alpha,{\lambda_1}^*)$.

The relation (A2.5) can be rewritten by using a characteristic toughness k_0':

$$\ln P_s = -\left[\frac{k_1}{k_0'(r_c)}\right]^m \quad \text{with} \quad k_0'(r_c) = \sigma_0\left[\frac{V_0}{B\Lambda_\theta}\right]^{1/m} r_c^{(m\lambda_1^*-2)/m} \tag{A2.5}$$

References

1. Singhal, S. C. and Kendall, K., *High Temperature Solid Oxide Fuel Cell: Fundamentals, Design, Applications*. Elsevier, Oxford, 2003.
2. Damani, R., Gstrein, R. and Danzer, R., Critical notch-root radius effect in SENB-S fracture toughness testing. *J. Eur. Ceram. Soc.*, 1996, **16**, 695–702.
3. J. Kübler, ESIS TC6, Round robin on fracture toughness of ceramics using the SEVNB method, Vamas Report No. 37, ESIS Document D2-99; September 1999.
4. Hertel, D., Fett, T. and Munz, D., Strength predictions for notched alumina specimens. *J. Eur. Ceram. Soc.*, 1998, **18**, 329–338.
5. Towse, A., Potter, K. D., Wisnom, M. R. and Adams, R. D., The sensitivity of a Weibull failure criterion to singularity strength and local geometry variations. *Int. J. Adhes. Adhes.*, 1999, **19**, 71–87.
6. Afferante, L., Ciavarella, M. and Valenza, E., Is Weibull's modulus really a material constant? Example case with interacting collinear cracks. *Int. J. Solids Struct.*, 2006, **43**, 5147–5157.
7. O'Dowd, N. P., Lei, Y. and Busso, E. P., Prediction of cleavage failure probabilities using the Weibull stress. *Eng. Fract. Mech.*, 2000, **67**, 87–100.
8. Lamon, J., Statistical approaches to failure for ceramic reliability assessment. *J. Am. Ceram. Soc.*, 1988, **71**(2), 106–112.
9. Evans, A. G., A general approach for the statistical analysis of multiaxial fracture. *J. Am. Ceram. Soc.*, 1977, **61**(7–8), 302–308.
10. Matsuo, Y., A probabilistic analysis of the brittle fracture loci under bi-axial stress state. *Bull. JSME*, 1981, **24**(188), 290–294.
11. Weibull, W., A statistical distribution function of wide applicability. *J. Appl. Mech.*, 1951, **18**(3), 293–297.
12. Wachtman, John B., *Mechanical Properties of Ceramics*. Wiley, New York, 1996, pp. 89–115.
13. Batdorf, S. B. and Crose, J. G., A statistical theory for the fracture of brittle structures subjected to polyaxial stress states. *J. Appl. Mech.*, 1974, **41**, 459–465.
14. Kassir, M. K. and Sih, G. C., Three-dimensional stress distribution around an elliptical crack under arbitrary loadings. *J. Appl. Mech.*, 1966, **33**(3), 601–611.
15. Thiemeier, T., Brückner-Foit, A. and Kölker, H., Influence of the fracture criterion on the failure prediction of ceramics loaded in biaxial flexure. *J. Am. Soc.*, 1991, **74**(1), 48–52.
16. Brückner-Foit, A., Fett, T., Schirmer, K.-S. and Munz, D., Discrimination of multiaxiality criteria using brittle fracture loci. *J. Eur. Ceram. Soc.*, 1996, **16**, 1201–1207.
17. http://www-cast3m.cea.fr/cast3m/index.jsp.
18. Leguillon, D. and Sanchez-Palencia, E., *Computation of Singular Solutions in Elliptic Problems and Elasticity*. J. Wiley, New York/Masson, Paris, 1987.
19. Williams, M. L., Stress singularities resulting from various boundary conditions in angular corners of plates in tension. *J. Appl. Mech.*, 1952, **19**, 526–528.
20. Lei, Y., O'Dowd, N. P., Busso, E. P. and Webster, G. A., Weibull stress solutions for 2-D cracks in elastic and elastic-plastic materials. *Int. J. Fract.*, 1998, **89**, 245–268.
21. Filippi, S., Lazzarin, P. and Tovo, R., Developments of some explicit formulas useful to describe elastic stress fields ahead of notches in plates. *Int. J. Solids Struct.*, 2002, **39**, 4543–4565.
22. Atzori, B., Lazzarin, P. and Filippi, S., Cracks and notches: analogies and differences on the relevant stress distribution and practical consequences in fatigue limit predictions. *Int. J. Fatigue*, 2001, **23**, 355–362.
23. Atkinson, A. and Selçuk, A., Mechanical behaviour of ceramic oxygen ion-conducting membranes. *Solid State Ionics*, 2000, **134**, 59–66.
24. Selçuk, A. and Atkinson, A., Strength and toughness of tape cast yttria stabilized zirconia. *J. Am. Soc.*, 2000, **83**(8), 2029–2035.
25. Picard, D., Leguillon, D. and Putot, C., A method to estimate the influence of the notch-root radius on the fracture toughness measurement of ceramics. *J. Eur. Ceram. Soc.*, 2006, **26**, 1421–1427.
26. Anderson, T. L., *Fracture Mechanics Fundamentals and Applications* (*second ed.*). CRC Press, New York, 1995, pp. 38–41.
27. Griffith, A. A., The phenomena of rupture and flaw in solids. *Philos. Trans. R. Soc. A*, 1920, **221**, 163–198.